

Cyclopentadienyl Tantalum(V) Complexes with Primary and Secondary Ferrocenylphosphine Ligands

René Kalio^a, Peter Lönnecke^a, Arnaldo Cinquantini^b, Piero Zanello^b, and Evamarie Hey-Hawkins^{a,*}^a Leipzig/Germany, Institut für Anorganische Chemie der Universität^b Siena/Italy Dipartimento di Chimica dell'Università di Siena

Received July 14th, 2007.

Dedicated to Professor Dieter Fenske on the Occasion of his 65th Birthday

Abstract. The reaction of $[\text{Cp}^*\text{TaCl}_4]$ (**1a**, $\text{Cp}^* = \text{C}_5\text{Me}_5$) or $[\text{Cp}'\text{TaCl}_4(\text{THF})]$ (**1b**, $\text{Cp}' = \text{C}_5\text{MeH}_4$) with PH_2Fc [$\text{Fc} = \text{Fe}(\eta^5\text{-C}_5\text{H}_5)(\eta^5\text{-C}_5\text{H}_4)$] and $\text{PH}_2\text{CH}_2\text{Fc}$ gives the primary ferrocenylphosphine complexes $[\text{Cp}^R\text{TaCl}_4(\text{PH}_2\text{Fc})]$ [$\text{Cp}^R = \text{Cp}^*$ (**2a**), Cp' (**2b**)] and $[\text{Cp}^R\text{TaCl}_4(\text{PH}_2\text{CH}_2\text{Fc})]$ [$\text{Cp}^R = \text{Cp}^*$ (**3a**), Cp' (**3b**)], respectively. **1** reacts with $(\text{PH}_2)_2\text{fc}$ [$\text{fc} = \text{Fe}(\eta^5\text{-C}_5\text{H}_4)_2$] or with the new secondary phosphine $\text{PH}(\text{CH}_2\text{Fc})_2$ to give the ferrocenyl-bridged complexes $\{[\text{Cp}^R\text{TaCl}_4][\text{PH}_2(\eta^5\text{-C}_5\text{H}_4)]_2\text{Fc}\}$ [$\text{Cp}^R = \text{Cp}^*$ (**4a**), Cp' (**4b**)] or $[\text{Cp}^R\text{TaCl}_4\{\text{PH}(\text{CH}_2\text{Fc})_2\}]$ [$\text{Cp}^R = \text{Cp}^*$ (**5a**), Cp' (**5b**)].

Complexes **1b** and **2–5** were characterised spectroscopically (^1H , ^{13}C , ^{31}P NMR, MS, IR) and **1b**, **2a**, **3a**, **4a**, and **5a** also by X-ray crystallography. The electrochemical behaviour of complexes **3a** and **5b** exhibits complicated electron transfer processes, which are due to the complex redox activity of the corresponding ferrocenylphosphine ligands $\text{PH}_2\text{CH}_2\text{Fc}$ and $\text{PH}(\text{CH}_2\text{Fc})_2$.

Keywords: Tantalum; Ferrocenylphosphines; ^{31}P NMR spectroscopy; Electrochemistry

Introduction

Organometallic dialkyl- and diarylphosphanido complexes of early transition metals have been studied intensively, while complexes derived from functionalized phosphines which have a reactive phosphorus–ligand bond have been largely neglected [1] due to the toxicity and high reactivity of the free phosphines (some are even pyrophoric). This lack of attention has prompted the development of primary and secondary phosphines that are more air-stable and hence easier to use [2–8]. Interest in these phosphines has arisen from the possibility of post-coordination modification of the P–H bond, which allows for chemical flexibility in the synthesis of new and intriguing transition metal phosphine complexes [9]. A recent development in the stabilisation of primary [2–4] and secondary [10, 11] phosphines has been the use of the ferrocenylmethyl fragment. Due to the redox properties of the ferrocenyl unit and the possibility to obtain chiral compounds readily, ferrocenylphosphines are an important class of ligands in transition metal chemistry [12]. In addition, ferrocene derivatives usually show enhanced stability and are generally non-toxic. Thus, their industrial applications range from additives for

heating oil to reduce formation of soot, iron-containing fertilisers, UV absorbers and protective coatings for rockets and satellites [12].

To date, only a few phosphanido derivatives of organometallic [13–15] and inorganic [16, 17] niobium and tantalum compounds, diphosphinediyl complexes [18], one phosphinidene-bridged dimeric Ta^{IV} complex [14] and two stable terminal phosphinidene complexes [17, 19] have been described in the literature, although potential starting materials such as cyclopentadienyl-substituted metal halides, alkyls, hydrides and carbonyls [20] are accessible, as are inorganic metal halides [21]. We expect cyclopentadienyl tantalum chloride complexes with primary or secondary phosphines to be suitable precursors for tantalum phosphanido or phosphinidene complexes, based on our work on the reactions of Zr and Mo complexes with primary phosphines or alkali metal phosphanides [22, 23], where we could show that a wide variety of products is obtained, depending on the nature of the organic substituents on phosphorus and the transition metal.

The Lewis acidity of tantalum(V) complexes has been extensively studied, and a large number of adducts of $[\text{Cp}^R\text{TaCl}_4]$ with ethers, amines, nitriles and isonitriles has been reported [24]. Up to now, only a few phosphine complexes of cyclopentadienyl tantalum tetrachloride are known, all but one of which have tertiary phosphine ligands [24d, 25–27]. We reported the synthesis of $[\text{Cp}'\text{TaCl}_4(\text{PH}_2\text{Tipp})]$ ($\text{Cp}' = \text{C}_5\text{MeH}_4$, $\text{Tipp} = 2,4,6\text{-Pr}^i_3\text{C}_6\text{H}_2$), which was the first cyclopentadienyl tantalum tetrachloride complex with a primary phosphine [14a], and a number of other tantalum and niobium complexes with

* Prof. Dr. E. Hey-Hawkins
Institut für Anorganische Chemie der Universität
Johannisallee 29
D-04103 Leipzig / Germany.
Fax: (0049)3419739319
Tel: (0049)3419736151
E-mail: hey@rz.uni-leipzig.de

primary phosphine ligands [28]. We have already shown that the phosphines PH_2Fc [$\text{Fc} = \text{Fe}(\eta^5\text{-C}_5\text{H}_5)(\eta^5\text{-C}_5\text{H}_4)$] [29], $\text{PH}_2\text{CH}_2\text{Fc}$ [3, 4] and $\text{PH}(\text{CH}_2\text{Fc})_2$ [10] ($= \text{L}$) react with transition metal complexes with reactive M-X bonds ($\text{X} = \text{halide}$) without loss of HX but with clean formation of the corresponding phosphine complexes, such as $[(p\text{-cymene})\text{RuCl}_2(\text{L})]$ ($p\text{-cymene} = 1\text{-Me-4-Pr}^i\text{C}_6\text{H}_4$) [3, 30, 31], $[\text{MI}_2(\text{CO})_3\text{L}_2]$, $[\text{MI}_2(\text{CO})_2\text{L}_3]$ ($\text{M} = \text{Mo, W}$) [32, 33, 34], and $[\text{WI}(\text{CO})_2\text{L}_4]\text{I}$ ($\text{L} = \text{PH}_2\text{CH}_2\text{Fc}$) [35].

We now report the synthesis of heterobimetallic di- and trinuclear organometallic tantalum complexes with primary or secondary ferrocenylphosphine ligands $[\text{Cp}^{\text{R}}\text{TaCl}_4\{\text{PH}_2(\text{CH}_2)_n\text{Fc}\}]$ [$n = 0$: $\text{Cp}^{\text{R}} = \text{Cp}^*$ (**2a**), Cp' (**2b**); $n = 1$: $\text{Cp}^{\text{R}} = \text{Cp}^*$ (**3a**), Cp' (**3b**)], $[\{(\text{Cp}^{\text{R}}\text{TaCl}_4)[\text{PH}_2(\eta^5\text{-C}_5\text{H}_4)]\}_2\text{Fe}]$ [$\text{Cp}^{\text{R}} = \text{Cp}^*$ (**4a**), Cp' (**4b**)] and $[\text{Cp}^{\text{R}}\text{TaCl}_4\{\text{PH}(\text{CH}_2\text{Fc})_2\}]$ [$\text{Cp}^{\text{R}} = \text{Cp}^*$ (**5a**), Cp' (**5b**)].

Results and Discussion

Synthesis

Starting materials

Recently, we published the crystal structure of $[\text{Cp}^*\text{TaCl}_4]$ (**1a**) [28], one of our starting materials, whose monomeric molecular structure is apparently due to the large Cp^* ligand. We therefore invested some effort in crystallising the related tantalum complex $[\text{Cp}'\text{TaCl}_4]$, whose Cp' ring is sterically less demanding, and which until today was only known as a yellow powder. While we could not crystallise the solvent-free complex $[\text{Cp}'\text{TaCl}_4]$, we obtained $[\text{Cp}'\text{TaCl}_4(\text{THF})]$ (**1b**) on recrystallisation of $[\text{Cp}'\text{TaCl}_4]$ from a mixture of diethyl ether with a small amount of THF. The crystal structure of **1b** is shown in Figure 1, and selected bond lengths and angles are listed in Table 1.

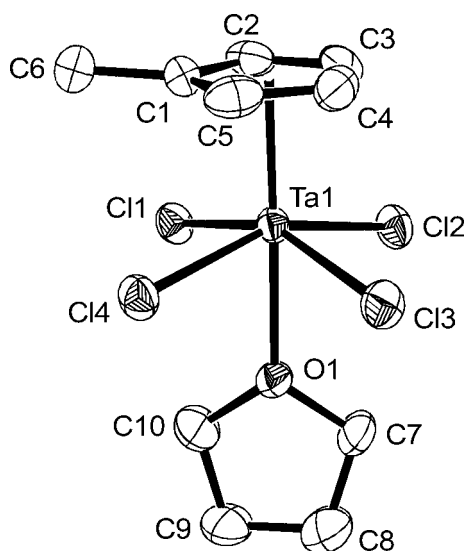


Fig. 1 Molecular structure of $[\text{Cp}'\text{TaCl}_4(\text{THF})]$ (**1b**).

Table 1 Selected bond lengths/pm and angles/ $^\circ$ in $[\text{Cp}'\text{TaCl}_4(\text{THF})]$ (**1b**) (CEN = C_5 centroid of the cyclopentadienyl ring)

Ta(1)-O(1)	231.3(4)
Ta(1)-Cl(3)	239.9(2)
Ta(1)-Cl(2)	240.4(2)
Ta(1)-Cl(4)	240.6(2)
Ta(1)-Cl(1)	241.4(2)
Ta(1)-CEN	212.1
O(1)-Ta(1)-CEN	178.5
Cl(1)-Ta(1)-CEN	101.9
Cl(2)-Ta(1)-CEN	103.3
Cl(3)-Ta(1)-CEN	103.8
Cl(4)-Ta(1)-CEN	102.0

As can be seen by comparison between **1a** and **1b**, coordination of the THF molecule to the tetragonal-pyramidal $[\text{Cp}'\text{TaCl}_4]$ fragment to give a six-coordinate octahedral complex results in a shortening of the distance between the equatorial plane of the four chloro ligands and the tantalum atom from 80.6 pm in **1a** to only 53.1 pm in **1b**.

Synthesis of tantalum ferrocenylphosphine complexes

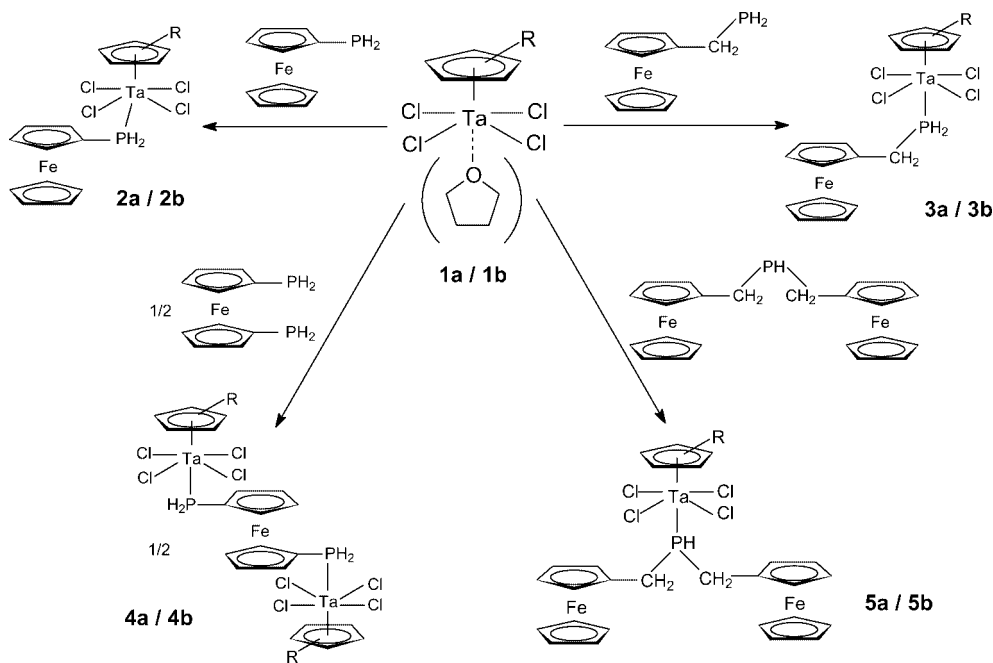
When an equimolar amount of the primary phosphines PH_2Fc , $\text{PH}_2\text{CH}_2\text{Fc}$ or the secondary phosphine $\text{PH}(\text{CH}_2\text{Fc})_2$ is added to complexes **1** in non-coordinating solvents like toluene or CH_2Cl_2 , complexes **2**, **3** and **5** can be isolated as orange or red crystals in high yields. The products are soluble in toluene, chloroform and dichloromethane, but hardly soluble in n -pentane or n -hexane. On addition of $(\text{PH}_2)_2\text{fc}$ ($\text{fc} = \text{Fe}(\eta^5\text{-C}_5\text{H}_4)_2$) to two equivalents of **1** the trinuclear products can be isolated as red crystals (**4a**) or a yellow powder (**4b**). The solubility of **4a** is much lower than that of the other complexes, and **4b** is almost insoluble in any common solvent. If the reaction between **1** and the ferrocenylphosphines is carried out in diethyl ether, the products form in poor yields and low purity, whereas use of THF often causes decomposition. In the solid state complexes **2-5** are quite stable in dry air (except for **3b**, which rapidly loses solvent), but in solution they decompose in a matter of hours if exposed to air.

Spectroscopic studies

Complexes **1b** and **2-5** were fully characterised by elemental analysis, infrared spectroscopy and NMR spectroscopy, the last-named mostly at low temperature. FAB mass spectrometry gave no molecular ion peak, but the fragment peaks could be unambiguously assigned, the heaviest mostly being the respective complex with loss of one or two chloro ligands or its adduct with the 3-nitrobenzyl alcohol matrix.

NMR spectroscopic investigations

As we already observed in previous investigations on tantalum phosphine complexes [28], the quadrupole momentum



Scheme 1 Reactions of $[\text{Cp}^*\text{TaCl}_4]$ and $[\text{Cp}'\text{TaCl}_4(\text{THF})]$ with the ferrocenylphosphines FcPH_2 , FcCH_2PH_2 , $\text{fc}(\text{PH}_2)_2$ and $(\text{FcCH}_2)_2\text{PH}$ to give the products **2–5** ($\text{Cp}^{\text{R}} = \text{Cp}^*$, Cp').

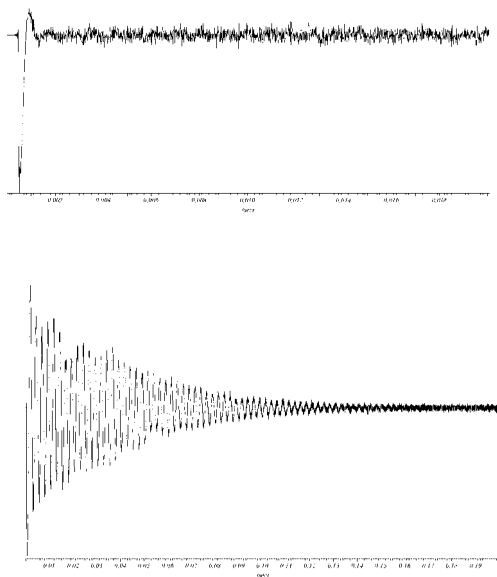


Fig. 2 ^{31}P NMR FIDs of $[\text{Cp}^*\text{TaCl}_4(\text{PH}_2\text{Fc})]$ (**2a**) in CDCl_3 recorded at $+25\text{ }^\circ\text{C}$ (first 20 ms, upper diagram) and at $-63\text{ }^\circ\text{C}$ (first 200 ms, lower diagram).

of the Ta atom causes extreme line broadening in the ^{31}P NMR spectra of the tantalum ferrocenylphosphine complexes at room temperature. The very short relaxation time at room temperature can be followed in the FID of the complexes (see Fig. 2). Nevertheless, it was possible to record ^{31}P NMR spectra of suitable quality at low temperature, except in cases of low solubility.

The ^{31}P NMR spectroscopic data of compounds **2–5** are shown in Table 2. As expected on coordination to a tran-

Table 2 ^{31}P NMR spectroscopic data of the tantalum complexes **2–5** recorded at $25\text{ }^\circ\text{C}$ in CDCl_3 , $\Delta\delta$ is the difference of the chemical shifts between the free ferrocenylphosphine and the respective complex.

	δ	$\Delta\delta$	$^1J_{\text{PH}}$
$[\text{Cp}^*\text{TaCl}_4(\text{PH}_2\text{Fc})]$ (2a)	-3.1 ppm	141.4 ppm	367 Hz *
$[\text{Cp}^*\text{TaCl}_4(\text{PH}_2\text{CH}_2\text{Fc})]$ (3a)	+1.2 ppm	130.3 ppm	359 Hz *
$\{[\text{Cp}^*\text{TaCl}_4][\text{PH}_2(\eta^5\text{-C}_5\text{H}_4)]\}_2\text{Fe}$ (4a)	-7.6 ppm	139.9 ppm	367 Hz *
$[\text{Cp}^*\text{TaCl}_4\{\text{PH}(\text{CH}_2\text{Fc})_2\}]$ (5a)	+38.5 ppm	91.9 ppm	375 Hz
$[\text{Cp}'\text{TaCl}_4(\text{PH}_2\text{Fc})]$ (2b)	-0.2 ppm	144.3 ppm	366 Hz
$[\text{Cp}'\text{TaCl}_4(\text{PH}_2\text{CH}_2\text{Fc})]$ (3b)	-2.7 ppm	126.4 ppm	372 Hz *
$\{[\text{Cp}'\text{TaCl}_4][\text{PH}_2(\eta^5\text{-C}_5\text{H}_4)]\}_2\text{Fe}$ (4b)	-3.3 ppm	144.2 ppm	375 Hz *
$[\text{Cp}'\text{TaCl}_4\{\text{PH}(\text{CH}_2\text{Fc})_2\}]$ (5b)	+43.5 ppm	96.9 ppm	377 Hz

* recorded at $-60\text{ }^\circ\text{C}$

sition metal, the signal of the phosphine ligand is shifted to low field compared to the free phosphine, by up to 147 ppm. This value is relatively high compared with previously described complexes of the type $[\text{Cp}^*\text{TaCl}_4(\text{PH}_2\text{R})]$ with $\text{R} = \text{Bu}^t$, adamantyl, Cy, Ph and Mes ($2,4,6\text{-Me}_3\text{C}_6\text{H}_2$), where the low field shift on coordination amounts to ca. 100–120 ppm. The $^1J_{\text{PH}}$ coupling constant increases by 160–180 Hz [28].

The differences in the chemical shift between the free phosphine and the respective tantalum(V) complex are larger for the primary ferrocenylphosphines than for the secondary $(\text{FcCH}_2)_2\text{PH}$. This could be due to increased shielding of the phosphorus atom when the primary phosphine ligand is coordinated to the $[\text{Cp}^{\text{R}}\text{TaCl}_4]$ fragment. On the other hand, the difference between the complexes with Cp^* and Cp' ligands is negligible ($\Delta\delta$ ca. 5 ppm).

Table 3 IR frequencies of the P–H stretching vibrations (in cm^{-1}) of complexes **2–5**.

Complex	$\nu(\text{P-H})$ (cm^{-1})
[Cp*TaCl ₄ (PH ₂ Fc)] (2a)	2399, 2378
[Cp*TaCl ₄ (PH ₂ CH ₂ Fc)] (3a)	2371
[{(Cp*TaCl ₄)[PH ₂ (η^5 -C ₅ H ₄)] ₂ Fe] (4a)	2388 (sh), 2365
[Cp*TaCl ₄ {PH(CH ₂ Fc) ₂ }] (5a)	2386
[Cp'TaCl ₄ (PH ₂ Fc)] (2b)	2389, 2369
[Cp'TaCl ₄ (PH ₂ CH ₂ Fc)] (3b)	2391
[{(Cp'TaCl ₄)[PH ₂ (η^5 -C ₅ H ₄)] ₂ Fe] (4b)	2387, 2364
[Cp'TaCl ₄ {PH(CH ₂ Fc) ₂ }] (5b)	2391

IR spectroscopy

The P–H stretching vibrations in the IR spectra of the tantalum complexes **2–5** have their absorption maxima between 2364 and 2399 cm^{-1} (see Table 3).

As expected, complexes **5a** and **5b** exhibit only one PH stretching band, while complexes **2a**, **2b**, **4a** and **4b** show two absorptions (ν_{as} and ν_{s} PH₂). However, unexpectedly, only one PH vibration is observed for **3a** and **3b**, as was previously also observed for some related tungsten and molybdenum complexes [34]. As is observed for other ferrocenylphosphine complexes [10, 30, 31, 33–35], the P–H stretching vibrations are shifted to higher wavenumbers compared to the free phosphines (PH₂Fc: 2225 cm^{-1} [29]; PH₂CH₂Fc: 2285 cm^{-1} [3]; PH(CH₂Fc)₂: 2285 cm^{-1} [10]).

X-ray structure determination

Molecular structures of [Cp*TaCl₄(PH₂Fc)] (**2a**), [Cp*TaCl₄(PH₂CH₂Fc)] (**3a**), [{(Cp*TaCl₄)[PH₂(η^5 -C₅H₄)]₂Fe] (**4a**) and [Cp*TaCl₄{PH(CH₂Fc)₂}] (**5a**)

Complex **2a** could be crystallised in two modifications under identical conditions (-30°C , from toluene). The solvent-free compound crystallises as dark red rhombohedra, whereas **2a**·0.5 toluene crystallises as dark red multilayered plates. Both modifications belong to the monoclinic space group $P2_1/c$.

Figure 3 illustrates the molecular structure of the solvent-free complex **2a**.

In the solvent-free complex the asymmetric unit comprises one molecule of the complex, while the asymmetric unit in the toluene solvate consists of two independent molecules of **2a** and one molecule of toluene. Although both structures appear to be very similar, packing effects cause large divergences in the bond lengths and angles of the two modifications (Table 4).

[Cp*TaCl₄(PH₂CH₂Fc)] (**3a**) was obtained as large, dark red prisms. The examined crystal contained two types of the molecule in a ratio of 70:30 %, apparently as enantiomers in different domains of the crystal (approximately mirror images, as shown in Fig 5.) The molecular structures of both types of molecule are shown in Figure 4; selected bond lengths and angles are given in Table 4.

[{(Cp*TaCl₄)[PH₂(η^5 -C₅H₄)]₂Fe] (**4a**) is located on a crystallographic inversion centre resulting in an antiperi-

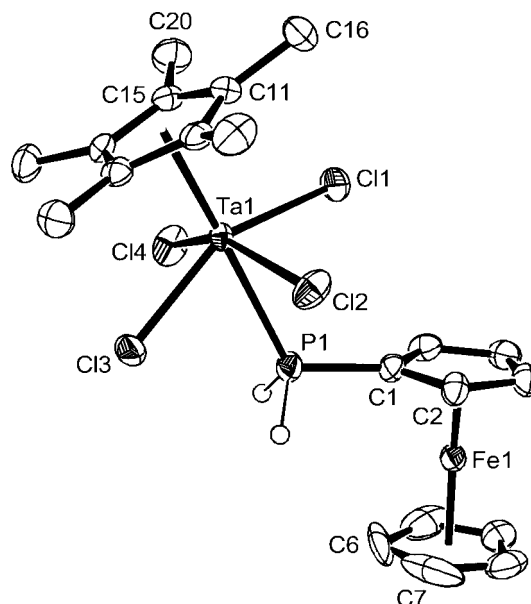


Fig. 3 Molecular structure of [Cp*TaCl₄(PH₂Fc)] (**2a**)

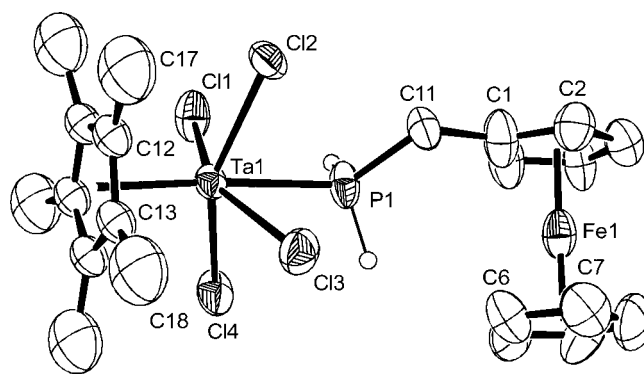


Fig. 4 Molecular structure of [Cp*TaCl₄(PH₂CH₂Fc)] (**3a**). Molecule from the 70 % domain shown.

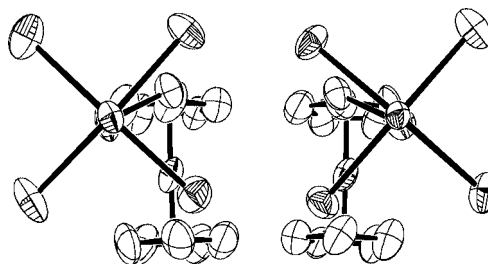


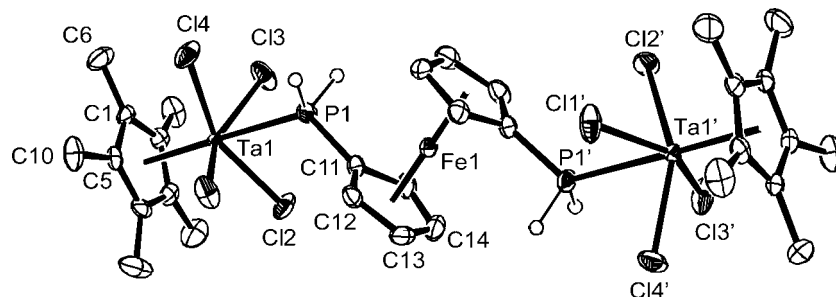
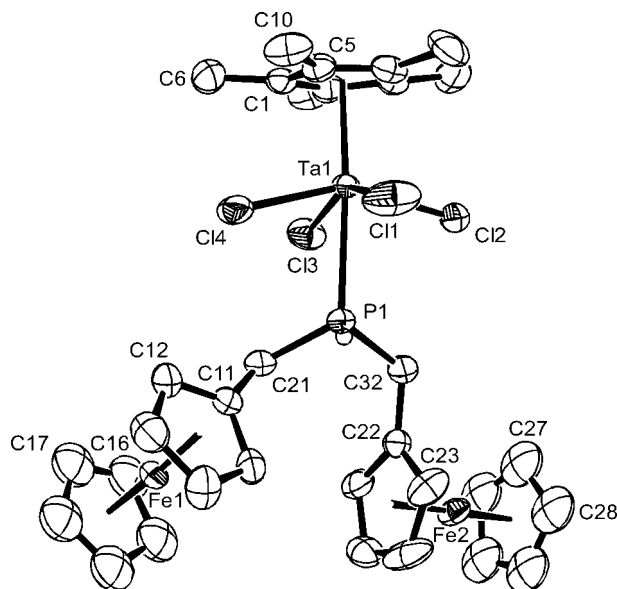
Fig. 5 The fragments [TaCl₄(PH₂CH₂Fc)] of the disordered molecules (70 % (left) and the 30 % domain (right) of **3a**) viewed from the centre of the C₅Me₅ rings. The C₅Me₅ rings and all H atoms have been left out for clarity.

planar arrangement of the two substituted cyclopentadienyl rings, as would be expected for bulky substituents in 1,1'-substituted ferrocenes (Fig. 6, Table 4) [12].

[Cp*TaCl₄{PH(CH₂Fc)₂}] (**5a**) was isolated as dark red crystals of the toluene solvate. **5a** crystallises in the mono-

Table 4 Selected bond lengths (pm) and angles ($^{\circ}$) of **2a**, **2b**, **3a**, **4a**, and **5a**.

Compound	2a ¹⁾	2a ·0.5 toluene ²⁾	3a ³⁾	4a	5a
Ta(1)-Cl(1)	239.0(1)	239.7(2), 238.8(2)	241.2(7), 241.8(3)	240.9(1)	241.5(3)
Ta(1)-Cl(2)	240.1(1)	238.5(2), 241.2(2)	239.6(7), 240.4(3)	238.1(1)	239.3(2)
Ta(1)-Cl(3)	241.4(1)	241.3(2), 239.2(2)	243.4(7), 243.2(3)	241.3(1)	240.4(3)
Ta(1)-Cl(4)	242.9(1)	241.0(2), 240.6(2)	242.3(7), 241.4(3)	242.3(1)	241.6(2)
Ta(1)-C(Cp ^R)	244.6(3)- 251.4(3)	241.3(2)- 250.6(7), 243.5(6)- 252.4(6)	248(2)- 267(3), 242.2(14)- 251.7(10)	244.2(5)- 250.5(5)	245.6(9)- 251.3(9)
Ta-CEN(Cp ^R) ⁴⁾	216.8	216.1, 215.9	221.0, 216.5	216.6	217.4
Ta-(mean plane 4 Cl)	61.1	61.7, 60.9	58.6, 60.6	61.3	59.5
Ta(1)-P(1)	264.7(1)	265.5(2), 264.8(2)	265.6(7), 265.9(3)	265.2(1)	267.7(2)
P(1)-C	179.6(3)	180.6(7), 177.7(7)	190(3), 183.0(11)	179.4(5)	182.2(9), 184.5(9)
Cl(1)-Ta(1)-Cl(2)	88.3(1)	89.84(9), 87.43(9)	87.5(3), 85.07(12)	87.77(6)	84.8(1)
Cl(1)-Ta(1)-Cl(3)	150.7(1)	150.38(7), 150.57(7)	151.2(2), 150.58(11)	150.37(5)	150.2(1)
Cl(2)-Ta(1)-Cl(3)	88.1(1)	86.3(1), 86.08(8)	85.3(3), 86.84(12)	86.01(6)	87.6(1)
Cl(1)-Ta(1)-Cl(4)	84.5(1)	85.47(7), 86.9(1)	87.1(3), 86.03(14)	86.37(6)	85.1(1)
Cl(2)-Ta(1)-Cl(4)	150.5(1)	149.96(7), 150.61(7)	152.6(2), 151.26(11)	150.62(5)	152.5(1)
Cl(3)-Ta(1)-Cl(4)	84.5(1)	83.40(8), 84.81(9)	86.6(3), 87.64(12)	85.02(7)	88.6(1)
Cl(1)-Ta(1)-P(1)	78.1(1)	73.84(6), 72.96(7)	77.6(2), 77.13(11)	72.60(5)	77.4(1)
Cl(2)-Ta(1)-P(1)	73.2(1)	73.64(6), 73.35(7)	78.7(2), 77.87(10)	75.93(5)	79.1(1)
Cl(3)-Ta(1)-P(1)	72.2(1)	76.90(6), 77.67(6)	73.7(2), 73.52(12)	77.79(5)	72.9(1)
Cl(4)-Ta(1)-P(1)	77.3(1)	76.55(6), 77.42(7)	73.9(2), 73.52(10)	74.85(5)	73.8(1)
C-P(1)-Ta(1)	120.4(1)	121.0(2), 121.9(2)	118.2(8), 119.5(4)	123.0(2)	117.7(3), 117.5(3)
C-P(1)-C	—	—	—	—	105.2(4)

¹⁾ solvent-free modification of **2a**²⁾ two independent molecules are present in the asymmetric unit³⁾ 30 % and 70 % domain⁴⁾ CEN = C₅ centroid of the Cp^R ring**Fig. 6** ORTEP plot of $\{[(\text{Cp}^*\text{TaCl}_4)[\text{PH}_2(\eta^5\text{-C}_5\text{H}_4)]_2\text{Fe}]\}$ (**4a**). All H atoms (except PH) are omitted for clarity.**Fig. 7** Molecular structure of $[\text{Cp}^*\text{TaCl}_4\{\text{PH}(\text{CH}_2\text{Fc})_2\}] \cdot \text{toluene}$ (**5a**·toluene). All H atoms (except PH) and the solvent molecule are omitted for clarity.

clinic space group $P2_1/c$. The molecular structure is illustrated in Figure 7, selected bond lengths and angles of complex **5a** are given in Table 4. In the crystal the ferrocenyl groups exhibit considerable distortion, which apart from packing effects seems to result from the steric influence of these bulky groups on each other. Free rotation of these voluminous groups is hindered even in solution, as indicated by two signals for the CH₂ groups in the ¹H NMR spectrum ($\Delta\delta = 0.51$ ppm in **5a**, 0.47 ppm in **5b**).

General features

All complexes **2a**, **3a**, **4a**, and **5a** (Fig. 3–7, Table 4) show a slightly distorted octahedral environment around the Ta atom, the axial positions of which are occupied by the centroid of the C₅ ring and the phosphine ligand. The chloro ligands arrange themselves in the equatorial plane, but are tilted away from the Cp* ligand.

As expected the $[\text{Cp}^*\text{TaCl}_4]$ fragments point away from the iron atom of the ferrocenyl group in all complexes.

By comparing the bond lengths and angles we were able to obtain a coherent picture of the steric influence

of different phosphine ligands on the geometry of the complex molecules. The Ta–P bond length is mainly influenced by electronic effects of the phosphine, and the Ta–P–C bond angles are reduced considerably in $[\text{Cp}^*\text{TaCl}_4\{\text{PH}(\text{CH}_2\text{Fc})_2\}]$ (**5a**, 117.5° and 117.7°) compared with other known complexes of the type $[\text{Cp}^R\text{TaCl}_4(\text{PH}_2\text{R})]$, which exhibit angles in the range between 119.5° and 131.0° .

Electrochemical studies on FcCH_2PH_2 and $(\text{FcCH}_2)_2\text{PH}$ and their complexes $[\text{Cp}^*\text{TaCl}_4(\text{PH}_2\text{CH}_2\text{Fc})]$ (**3a**) and $[\text{Cp}^*\text{TaCl}_4\{\text{PH}(\text{CH}_2\text{Fc})_2\}]$ (**5b**)

The difficulties encountered in interpreting the electrochemical behaviour of mono- and diferrocenylphosphines of the types FcCH_2PR_2 and $(\text{Fc})_2\text{PR}$ are well established [36, 37]. They usually afford responses complicated by electrode adsorption phenomena and/or chemical complications. The present ferrocenylphosphines FcCH_2PH_2 and $(\text{FcCH}_2)_2\text{PH}$ give rise to even more complicated electrochemical responses, which are in turn reflected in the redox behaviour of the complexes $[\text{Cp}^*\text{TaCl}_4(\text{PH}_2\text{CH}_2\text{Fc})]$ (**3a**) and $[\text{Cp}^*\text{TaCl}_4\{\text{PH}(\text{CH}_2\text{Fc})_2\}]$ (**5b**). In fact, unexpectedly, a CH_2Cl_2 solution of FcCH_2PH_2 displays a first, partially chemically reversible, oxidation ($[\text{FcCH}_2\text{PH}_2]^{0/+}$; $E^{0'}$ = $+0.35$ V, vs. SCE), followed by further closely spaced oxidations arising from chemical complications following the first step, the main of which is tentatively attributed to the oxidation of the byproduct $[\text{FcCH}_2\text{OH}]$ ($E^{0'}$ = $+0.42$ V) [38]. Since it is known that hydridic hydrogen atoms in metal complexes undergo anodic oxidation [39], the generation of the mentioned byproduct likely occurs from the partial stability of $[\text{FcCH}_2\text{PH}_2]^+$, which triggers oxidative elimination of hydrides, breakage of the C–P bond, and insertion of an OH group from the nominally anhydrous solution.

We note that such behaviour is in sharp contrast with that of $\text{FcCH}_2\text{PPh}_2$, which exhibits a chemically reversible one-electron oxidation accompanied by slight adsorption phenomena [40].

In confirmation of the complex oxidation pattern, coulometric measurements corresponding to the overall oxidation process (E_w = $+0.7$ V) showed the consumption of three electrons per molecule. In fact, the original yellow solution does not show any colour change after about one electron *per* molecule, turns green after about two electrons *per* molecule (as a consequence of the spectrally supported generation of $[\text{FcCH}_2\text{OH}]^+$) and blue after about three electrons *per* molecule.

This being stated, let us consider the cyclic voltammetric profile of the oxidation path of the monoferrocenyl complex $[\text{Cp}^*\text{TaCl}_4(\text{PH}_2\text{CH}_2\text{Fc})]$ (**3a**) at a platinum and at a glassy carbon electrode, respectively. As far as the cathodic region is concerned, an irreversible tantalum(V)-centred reduction (not shown in Figure 8) is also present ($E_p \approx -0.7$ V), which is ill defined probably because of electrode-poisoning phenomena.

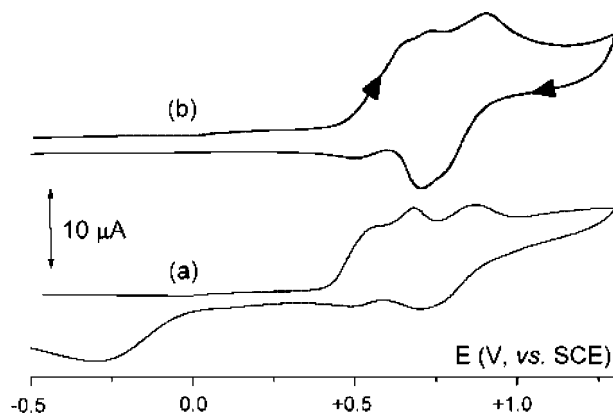


Figure 8 Cyclic voltammograms recorded in CH_2Cl_2 solution of $[\text{Cp}^*\text{TaCl}_4(\text{PH}_2\text{CH}_2\text{Fc})]$ (**3a**) (0.9×10^{-3} mol dm^{-3}), $[\text{NBu}_4][\text{PF}_6]$ (0.2 mol dm^{-3}) supporting electrolyte. (a) Platinum electrode; (b) glassy carbon electrode. Scan rate 0.2 Vs^{-1} .

The use of the two electrode materials confirmed that the overall oxidation process is accompanied by release of protons. In fact, since the reduction of protons at the glassy carbon electrode is shifted towards very negative potentials with respect to the standard electrode potentials of the H_2/H^+ couple [41], the presence of the backscan peak at $E_p = -0.26$ V at the platinum electrode confirms the hypothesis.

It is hence concluded that also in this case the first step ($E^{0'} = +0.50$ V in Osteryoung square-wave voltammetry) of the three ferrocenyl-centred oxidations triggers decoordination followed by the previously illustrated anodic path of the released ferrocenyl ligand.

Figure 9 finally shows the cyclic voltammetric pattern for the oxidation of the diferrocenyl complex $[\text{Cp}^*\text{TaCl}_4\{\text{PH}(\text{CH}_2\text{Fc})_2\}]$ (**5b**), also in comparison with that of the free ligand $(\text{FcCH}_2)_2\text{PH}$.

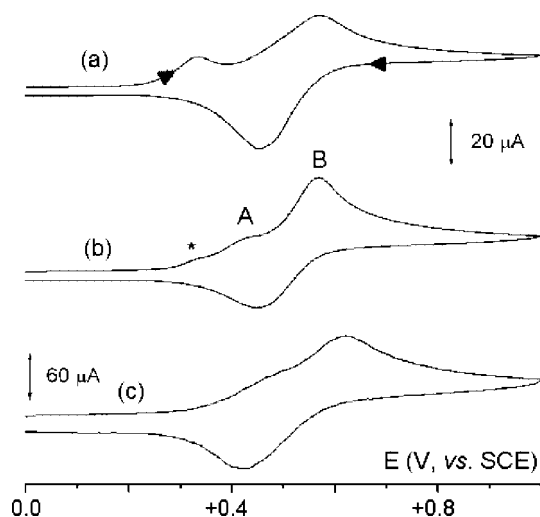


Figure 9 Cyclic voltammograms recorded at a platinum electrode in CH_2Cl_2 solution of: (a) $(\text{FcCH}_2)_2\text{PH}$ (0.8×10^{-3} mol dm^{-3}); (b, c) $[\text{Cp}^*\text{TaCl}_4\{\text{PH}(\text{CH}_2\text{Fc})_2\}]$ (**5b**) (0.6×10^{-3} mol dm^{-3}), $[\text{NBu}_4][\text{PF}_6]$ (0.2 mol dm^{-3}) supporting electrolyte. Scan rates: (a, b) 0.2 Vs^{-1} ; (c) 2.0 Vs^{-1} .

The response of $(\text{FcCH}_2)_2\text{PH}$ is qualitatively reminiscent of that of $(\text{FcCH}_2)_2\text{PPh}$ under the same experimental conditions [37a], i.e. a relatively broad, two-electrons oxidation with features of chemical reversibility ($E^{\circ'} = +0.51\text{ V}$; $\Delta E_p = 120\text{ mV}$ at 0.2 Vs^{-1}) which is preceded by a prewave typical of strong adsorption of the electron-transfer product ($E_p = +0.33\text{ V}$) [40]. At variance with the latter, exhaustive electrolysis of $(\text{FcCH}_2)_2\text{PH}$ consumes six electrons *per* molecule. As in the case of FcCH_2PH_2 , the yellow colour of the original solution remains unchanged in the first stages of the oxidation process (up to about 1.5 electrons per molecule), then progressively turns green and blue. Concomitantly, in confirmation of the cited adsorption phenomena, a blue deposit appears on the electrode surface. The final species remaining in solution exhibits a reversible reduction at $+0.40\text{ V}$.

In turn, the tantalum complex shows two closely spaced oxidations, which are not resolved even in Osteryoung square-wave voltammetry (peak A, $E_p \approx +0.4\text{ V}$; peak B, $E^{\circ'} = +0.54\text{ V}$) and are preceded by a very minor peak (marked with *), which coincides with the adsorption prewave of the free ligand. In the backscan profile (not shown in Figure 9) a reduction around -0.2 V also appears which, since it takes place only at the platinum electrode, is assigned to proton reduction. As illustrated in Figure 9c, upon increasing the scan rate, the second anodic process tends to decrease, thus indicating that it arises from chemical complications following the first anodic step. Finally, the tantalum(V)-centred reduction is also detected at -0.69 V upon direct scan towards negative potentials.

Unfortunately, we did not succeed in determining the number of electrons involved in the overall oxidation pro-

cess, since after the consumption of about two electrons per molecule the electrolysis current suddenly dies out. Since the cyclic voltammetric profile remains substantially unchanged with respect to the original one, we attribute the current breaking to electrode-poisoning phenomena.

In conclusion, the ferrocenylphosphines FcCH_2PH_2 and $(\text{FcCH}_2)_2\text{PH}$ undergo complicated oxidation processes which are substantially reflected in the anodic behaviour of their tantalum(V) complexes $[\text{Cp}^*\text{TaCl}_4(\text{PH}_2\text{CH}_2\text{Fc})]$ (**3a**) and $[\text{Cp}^*\text{TaCl}_4\{\text{PH}(\text{CH}_2\text{Fc})_2\}]$ (**5b**). This also holds for the pertinent redox potentials, that is, the tantalum complex fragment does not substantially affect the electronic situation of the ferrocenyl ligands.

Subsequent reactions of complexes 2–5

Apart from attempting to prepare suitable starting materials for the preparation of phosphanido and phosphinidene complexes we observed spontaneous reactions between the complexes and the solvent which emphasize the high reactivity of the P–H bond in the tantalum primary phosphine complexes.

On dissolving complexes of the type $[\text{Cp}^*\text{TaCl}_4(\text{PH}_2\text{R})]$ in CDCl_3 proton/deuterium exchange could be observed at the PH_2 groups of the phosphine ligand of complexes **2a**, **2b**, **3a** and **5b**. In the ^{31}P NMR spectrum the PHD groups gave the typical 1:1:1 triplet in which the $^1J(^{31}\text{P}^2\text{H})$ coupling constant is ca. 15% of the $^1J(^{31}\text{P}^1\text{H})$ coupling constant of the PH_2 group [42] (Fig. 10).

Scheme 2 shows the H/D exchange reaction with deuterated protic solvents.

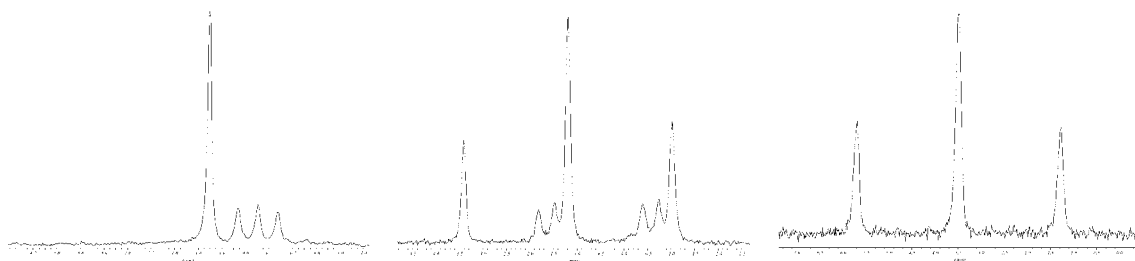
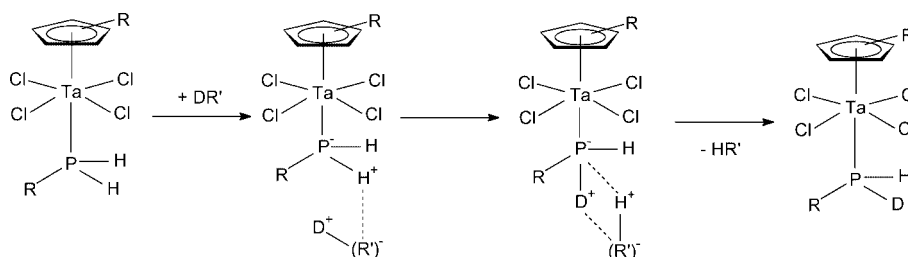


Fig. 10 ^{31}P NMR spectra of $[\text{Cp}^*\text{TaCl}_4(\text{PH}_2\text{CH}_2\text{Fc})]$. Left: Proton-decoupled spectrum in CDCl_3 . Apart from the singlet of the educt a 1:1:1 triplet due to $^1J(\text{PD})$ coupling of the H-D exchange product $[\text{Cp}^*\text{TaCl}_4\{(\text{PHD})\text{CH}_2\text{Fc}\}]$ can be seen. Centre: Proton-coupled spectrum in CDCl_3 . $^1J(\text{PH})$ coupling gives a triplet for the unchanged complex which overlaps with a doublet of 1:1:1 triplets for the exchange product. Right: Proton-coupled spectrum in CHCl_3 .



Scheme 2 H-D exchange reaction between $[\text{Cp}^*\text{TaCl}_4(\text{PH}_2\text{R})]$ and deuterated protic solvents (DR).

Experimental Section

General

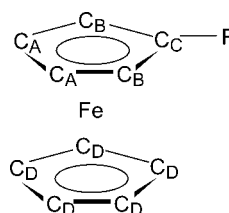
All manipulations were carried out with standard high-vacuum and dry-nitrogen techniques. Solvents were purified and dried according to standard procedures. NMR spectra: Avance DRX 400 (Bruker), standards: ^1H NMR (400 MHz): TMS, ^{13}C NMR (100.6 MHz): TMS, ^{31}P NMR (162 MHz): external 85% H_3PO_4 . ^{31}P NMR data of **2–5** are given in Table 2. The IR spectra were recorded as KBr disks on a Perkin-Elmer System 2000 FT-IR spectrometer in the range 350–4000 cm^{-1} . Mass spectra were obtained with a Varian MAT 711 Spectrometer (FAB, 70 eV, source temperature 180 °C, 3-NBA matrix). The melting points were determined in sealed capillaries and are uncorrected. PH_2Fc [29], $\text{PH}_2\text{CH}_2\text{Fc}$ [3, 4], $\text{PH}(\text{CH}_2\text{Fc})_2$ [10], $[\{\text{PH}_2(\eta^5\text{-C}_5\text{H}_4)\}_2\text{Fe}]$ [43], $[\text{Cp}^*\text{TaCl}_4]$ [24b], and $[\text{Cp}^*\text{TaCl}_4]$ [44] were prepared according to the literature. Materials and apparatus for electrochemistry and spectroelectrochemistry have been described elsewhere [45]. The potential values are referred to the Saturated Calomel Electrode (SCE). Under the present experimental conditions, the one-electron oxidation of ferrocene occurs at $E^{\circ'} = +0.39$ V.

X-Ray crystallography

In most cases it was possible to grow crystals suitable for X-ray crystallography, either by cooling a concentrated solution to -30 °C, or by evaporation of solvent under inert gas. Although crystals of **3b** could be grown at low temperature in CH_2Cl_2 , they disintegrated rapidly on exposure to room temperature or removal from the solvent, to form a grey or black, microcrystalline, apparently solvent-free modification, so that our attempts to structurally characterise the complex were unsuccessful. Attempts to grow crystals of **4b** were thwarted by its low solubility.

X-ray diffraction data were collected on a Siemens SMART CCD diffractometer (radiation: $\text{MoK}\alpha$, $\lambda = 71.073$ pm; method: ω scans rotation). Absorption correction was performed using the program SADABS [46]. The structures were solved by direct methods, and all non-hydrogen atoms were refined anisotropically (SHELX97) [47]. H atoms were refined isotropically. The protons were calculated on idealised positions. The thermal ellipsoids in Figs. 1 and 3–7 are shown with 50% probability. Crystal data and structure refinement for compounds **1b**, **2a**, **3a**, **4a**, and **5a** are given in Table 5. CCDC 660554 **1b**, CCDC 660556 **2a**, CCDC 660555 **2a**·0.5 toluene, CCDC 660557 **3a**, CCDC 660553 **4a**, and 660558 **5a** contain the supplementary crystallographic data for this paper. These data can be obtained free of charge via www.ccdc.cam.ac.uk/conts/retrieving.html (or from the Cambridge Crystallographic Data Centre, 12 Union Road, Cambridge CB2 1EZ, UK; fax: (+44)1223-336-033; or deposit@ccdc.cam.ac.uk).

The atom labelling scheme for the NMR assignments is as follows ($\text{R} = \text{PH}_2$, CH_2PH_2 or $\text{CH}_2\text{P}(\text{H})\text{CH}_2\text{Fc}$):



Preparations

[Cp*TaCl₄(THF)] (1b). $[\text{Cp}^*\text{TaCl}_4]$ was recrystallised from diethyl ether to which a stoichiometric amount of THF was added (ca. 0.2 g THF for 1 g $[\text{Cp}^*\text{TaCl}_4]$). The crystalline yellow product **1b** was obtained in almost quantitative yield. Mp: dec. 65 °C,

Table 5 Crystal data and structure refinement for **1b** and **2–5**.

Complex	1b	2a	2a ·0.5 toluene	3a	4a	5a ·toluene
Empirical formula	$\text{C}_{10}\text{H}_{15}\text{Cl}_4\text{OTa}$	$\text{C}_{20}\text{H}_{26}\text{Cl}_4\text{FePTa}$	$\text{C}_{23.5}\text{H}_{30}\text{Cl}_4\text{FePTa}$	$\text{C}_{21}\text{H}_{28}\text{Cl}_4\text{FePTa}$	$\text{C}_{32}\text{H}_{46}\text{Cl}_{12}\text{FeP}_2\text{Ta}_2$	$\text{C}_{39}\text{H}_{46}\text{Cl}_4\text{Fe}_2\text{PTa}$
Formula weight	473.97	675.98	772.04	690.00	1335.78	980.18
Temperature	217(2) K	208(2) K	208(2) K	208(2) K	210(2) K	208(2) K
Crystal system	monoclinic	monoclinic	monoclinic	monoclinic	monoclinic	monoclinic
Space group	$P2_1/n$	$P2_1/c$	$P2_1/c$	$P2_1/c$	$C2/c$	Cc
Unit cell dimensions	a = 694.66(11) pm b = 2103.2(3) pm c = 968.19(16) pm $\beta = 105.487(3)^\circ$	a = 993.53(10) pm b = 1257.13(13) pm c = 1856.44(18) pm $\beta = 95.019(2)^\circ$	a = 1716.8(3) pm b = 859.44(15) pm c = 3528.3(6) pm $\beta = 91.946(3)^\circ$	a = 1316.7(3) pm b = 1113.7(2) pm c = 1696.8(3) pm $\beta = 104.276(4)^\circ$	a = 1274.10(7) pm b = 1205.62(7) pm c = 2896.6(2) pm $\beta = 98.947(1)^\circ$	a = 2027.53(10) pm b = 1719.70(10) pm c = 1221.13(6) pm $\beta = 115.2380(10)^\circ$
Volume	1.3632(4) nm^3	2.3098(4) nm^3	5.2030(16) nm^3	2.4112(8) nm^3	4.3952(4) nm^3	3.8513(3) nm^3
Z	4	4	8	4	4	4
Density (calculated)	2.309 g/cm^3	1.944 g/cm^3	1.844 g/cm^3	1.901 g/cm^3	2.019 g/cm^3	1.690 g/cm^3
Absorption coefficient	8.823 mm^{-1}	5.898 mm^{-1}	5.243 mm^{-1}	5.652 mm^{-1}	6.120 mm^{-1}	3.924 mm^{-1}
$F(000)$	896	1312	2824	1344	2576	1952
Crystal size	0.20 x 0.12 x 0.10 mm	0.10 x 0.10 x 0.05 mm	0.20 x 0.15 x 0.05 mm	0.20 x 0.10 x 0.05 mm	0.40 x 0.30 x 0.20 mm	0.20 x 0.10 x 0.04 mm
θ range for data collection	1.94–28.86°	1.96–28.98°	1.63–28.88°	2.21–28.97°	1.42–26.37°	1.62–29.00°
Index ranges	$-9 \leq h \leq 9$ $-27 \leq k \leq 28$ $-12 \leq l \leq 6$	$-13 \leq h \leq 13$ $-16 \leq k \leq 17$ $-24 \leq l \leq 9$	$-139 \leq h \leq 22$ $-9 \leq k \leq 11$ $-45 \leq l \leq 47$	$-15 \leq h \leq 17$ $-14 \leq k \leq 15$ $-22 \leq l \leq 17$	$-14 \leq h \leq 15$ $-14 \leq k \leq 15$ $-34 \leq l \leq 24$	$-18 \leq h \leq 27$ $-19 \leq k \leq 23$ $-16 \leq l \leq 13$
Reflections collected	8838	15043	32918	15615	9885	12593
Independent reflections	3275 [$R(\text{int}) = 0.0826$]	5610 [$R(\text{int}) = 0.0406$]	12526 [$R(\text{int}) = 0.0816$]	5824 [$R(\text{int}) = 0.1060$]	3999 [$R(\text{int}) = 0.0246$]	6588 [$R(\text{int}) = 0.0580$]
Completeness to θ_{max}	to $\theta = 28.86^\circ$: 91.6%	to $\theta = 28.98^\circ$: 91.5%	to $\theta = 28.88^\circ$: 91.7%	to $\theta = 28.97^\circ$: 91.2%	to $\theta = 26.37^\circ$: 89.5%	to $\theta = 29.00^\circ$: 91.2%
Max. and min. transmission	0.4724 and 0.2714	0.7569 and 0.5900	0.7795 and 0.4203	0.7653 and 0.3977	0.3741 and 0.1933	0.8588 and 0.5075
Data / restraints / parameters	3275 / 0 / 146	5610 / 0 / 273	12526 / 22 / 577	5824 / 74 / 293	3999 / 0 / 270	6588 / 3 / 386
Goodness-of-fit on F^2	1.043	0.984	0.965	0.855	1.247	1.001
Final R indices [$>2\sigma(I)$]	$R_1 = 0.0384$, $wR_2 = 0.1004$	$R_1 = 0.0267$, $wR_2 = 0.0548$	$R_1 = 0.0490$, $wR_2 = 0.1008$	$R_1 = 0.0600$, $wR_2 = 0.1217$	$R_1 = 0.0278$, $wR_2 = 0.0633$	$R_1 = 0.0416$, $wR_2 = 0.0912$
R indices (all data)	$R_1 = 0.0440$, $wR_2 = 0.1047$	$R_1 = 0.0376$, $wR_2 = 0.0574$	$R_1 = 0.0836$, $wR_2 = 0.1127$	$R_1 = 0.1280$, $wR_2 = 0.1364$	$R_1 = 0.0305$, $wR_2 = 0.0702$	$R_1 = 0.0548$, $wR_2 = 0.0995$
Absolute structure parameter	–	–	–	–	–	0.545(10)
Largest diff. peak and hole	1.864 and $-2.563 \text{ e } \text{\AA}^{-3}$	1.073 and $-0.867 \text{ e } \text{\AA}^{-3}$	2.655 and $-2.223 \text{ e } \text{\AA}^{-3}$	2.002 and $-1.169 \text{ e } \text{\AA}^{-3}$	0.874 and $-1.527 \text{ e } \text{\AA}^{-3}$	1.312 and $-1.311 \text{ e } \text{\AA}^{-3}$

¹H NMR (25 °C, CDCl₃): δ 2.08 (br s, 4H, THF), 2.97 (s, 3H, C₅H₄CH₃), 4.73 (vbr s, 4H, THF, OCH₂), 6.50 and 6.95 (2 m, C₅H₄); **¹H NMR** (−30 °C, CDCl₃): no change. **¹³C{¹H} NMR** (25 °C, CDCl₃): δ 17.3 (s, C₅H₄CH₃), 26.5 (s, THF), 71.4 (s, THF, OCH₂), 122.8 and 123.9 (2 s, C₅H₄), 136.6 (s, *ipso*-C in C₅H₄).

[Cp*TaCl₄(PH₂Fc)] (2a). PH₂Fc (0.12 g, 0.55 mmol) was added to a stirred solution of [Cp*TaCl₄] (0.25 g, 0.55 mmol) in toluene (10 mL). A brown precipitate formed slowly. After 24 h the solvent was evaporated in vacuum, and the residue washed with *n*-pentane and dried. Yield 0.36 g (97 %), yellow powder. Dark red crystals of solvent-free **2a** and/or **2a**·toluene can be obtained from a saturated toluene solution at −30 °C (after 1 d) or by slow diffusion of *n*-pentane into a toluene solution of **2a**. Mp (powder): dec. >194 °C (thermolysis to FePH₂ and [Cp*TaCl₄] as shown by IR spectra of the residue after thermolysis in vacuum). Anal. calc. for C₂₀H₂₆Cl₄FePtA (675.98): C, 35.54; H, 3.88; Cl, 20.60. Found: C, 35.89; H, 4.02; Cl, 20.60 %.

¹H NMR (25 °C, CDCl₃): δ 2.47 (s, 15H, CH₃), 4.23 (s, 5H, C₅H₅), 4.54 and 4.45 (2 s, each 2H, PH₂C₅H₄), 6.19 (br d, full width at half-maximum 0.05 ppm, ¹J_{PH} = 352 Hz, 2H, PH₂); at −63 °C, CDCl₃, the PH₂ signal occurs as a doublet at 6.41 (2H, full width at half-maximum 0.01 ppm, ¹J_{PH} = 367 Hz); **¹³C{¹H} NMR** (25 °C, CDCl₃): δ 13.3 (s, C₅(CH₃)₅), 66.1 (d, ¹J_{PC} = 33.4 Hz, PC in PH₂C₅H₄), 70.5 (s, C₅H₅), 71.8 (d, ³J_{PC} = 7.0 Hz, C_A in PH₂C₅H₄), 74.3 (d, ²J_{PC} = 8.7 Hz, C_B in PH₂C₅H₄), 133.3 (s, C₅(CH₃)₅); **³¹P NMR** (25 °C, C₆D₆ or CDCl₃): no signal observed; **³¹P{¹H} NMR** (25 °C, CDCl₃): −7.3 (vbr s, full width at half-maximum 9 ppm); **³¹P NMR** (−63 °C, CDCl₃): −3.1 (t, ¹J_{PH} = 367 Hz) (see Table 2); **MS**: m/z = 716.1 [Cp*TaCl₂(PH₂Fc)·3-NBA]⁺ (6.2 %), 420.8 [Cp*TaCl₃]⁺ (62.6 %), 384.9 [Cp*TaCl₂]⁺ (38.6 %), 218.1 [PH₂Fc]⁺ (79 %); **IR** (cm^{−1}): 3106 w, 2994 w, 2964 w, 2910 m, 2399 w, 2378 w, 1645 w, 1491 m, 1455 w, 1436 m, 1419 w, 1375 s, 1260 w, 1180 m, 1105 m, 1072 w, 1049 m, 1026 m, 1002 w, 896 w, 868 s, 841 m, 819 m, 686 w, 639 w, 596 w, 510 m, 488 m, 450 m, 421 w.

[Cp'TaCl₄(PH₂Fc)] (2b). Crystalline PH₂Fc (0.15 g, 0.69 mmol) was added to a stirred solution of [Cp'TaCl₄(THF)] (0.31 g, 0.65 mmol) in toluene (10 mL). The solution changed colour from orange to brown. After 24 h the solvent was evaporated in vacuum and the beige residue washed with pentane and dried. Yield: 0.38 g (94 %); mp: 191–192 °C (dec. >187 °C); Anal. calc. for C₁₆H₁₈Cl₄FePtA (619.90): C, 31.00; H, 2.93. Found: C, 31.13; H, 2.85 %.

¹H NMR (25 °C, CDCl₃): δ 2.82 (s, 3H, CH₃C₅H₄), 4.25 (s, 5H, C₅H₅), 4.43 and 4.55 (2 s, each 2H, PH₂C₅H₄), 6.49 (d, ¹J_{PH} = 378 Hz, 2H, PH₂), 6.35 (m (pseudotriplets), ³J_{HHH}/⁴J_{HHH} = 2.4 Hz, 2H, CH₃C₅H₄), 6.83 (m (pseudotriplets), ³J_{HHH}/⁴J_{HHH} = 2.6 Hz, 2H, CH₃C₅H₄); **¹³C{¹H} NMR** (25 °C, CDCl₃): δ 16.5 (s, CH₃C₅H₄), 65.7 (d, ¹J_{PC} = 36.7 Hz, P–C), 70.5 (s, C_D), 72.1 (d, ³J_{PC} = 7.0 Hz, C_A), 74.2 (d, ²J_{PC} = 7.8 Hz, C_B), 125.9 (s, CH₃CC₄ in CH₃C₅H₄), 125.1 (s, CH₃CC₄ in CH₃C₅H₄), 136.0 (s, CH₃–C in CH₃C₅H₄); **³¹P NMR** (25 °C, C₆D₆): δ −0.2 (t, vbr, ¹J_{PH} = 366 Hz); **MS**: m/z = 734.9 [Cp'TaCl₃(PFc)·3-NBA]⁺ (8 %), 584.9 [Cp'TaCl₃H(PH₂Fc)]⁺ (5.3 %), 581.0 [Cp'TaCl₃(PFc)]⁺ (5.3 %), 369.0 [Cp'TaCl₃]⁺ (10.5 %), 218.1 [PH₂Fc]⁺ (96.1 %); **IR** (cm^{−1}): 3103 m, 2950 w, 2918 w, 2389 w, 2369 w, 1496 m, 1449 m, 1410 m, 1385 w, 1375 m, 1360 w, 1265 w, 1249 w, 1180 m, 1105 m, 1078 w, 1050 m, 1027 m, 1001 m, 937 w, 895 m, 869 s, 818 m, 636 w, 613 w, 595 w, 485 m, 451 s.

[Cp*TaCl₄(PH₂CH₂Fc)] (3a). PH₂CH₂Fc (0.10 g, 0.43 mmol) was added to a solution of [Cp*TaCl₄] (0.19 g, 0.42 mmol) in toluene (10 mL). After 3 h the solution was concentrated in vacuum to 2 mL. At −30 °C large prismatic dark red crystals were obtained after 24 h. Yield: 0.20 g (69 %); mp: dec. >169 °C (thermolysis to PH₂CH₂Fc and [Cp*TaCl₄]); Anal. calc. for C₂₁H₂₈Cl₄FePtA (690.00): C, 36.55; H, 4.09. Found: C, 36.61; H, 4.41 %.

¹H NMR (25 °C, CDCl₃): δ 2.46 (s, 15H, CH₃), 3.20 (br s, 2H, PCH₂Fc), 4.14 and 4.19 (2 br s, 9H, Fe(η⁵-C₅H₅)(η⁵-C₅H₄)), 5.21 (br d, full width at half-maximum 0.01 ppm, ¹J_{PH} = 367 Hz, 2H, PH₂); **¹³C{¹H} NMR** (25 °C, CDCl₃): δ 13.4 (s, C₅(CH₃)₅), 68.7 and 69.0 (2 s, C_A and C_B in

PH₂CH₂C₅H₄), 69.7 (s, C₅H₅), 70.6 (s, C_C in PH₂CH₂C₅H₄), 19.7 (br, PH₂CH₂), 133.7 (s, C₅(CH₃)₅); **³¹P{¹H} NMR** (25 °C, CDCl₃): δ −1.4 (vbr s, full width at half-maximum 3 ppm); **³¹P NMR** (25 °C, CDCl₃): no signal; **³¹P{¹H} NMR** (−63 °C, CDCl₃): δ 1.2 (s, PH₂), 0.4 (PHD, 1:1:1 triplet, ¹J_{PD} = 55 Hz), ratio 1:0:6; **³¹P NMR** (−63 °C, CDCl₃): δ 1.2 (t, ¹J_{PH} = 359 Hz, PH₂), 0.4 (d of 1:1:1 triplet, ¹J_{PH} = 358 Hz (d), ¹J_{PD} = 56 Hz (1:1:1-t), PHD); **³¹P NMR** (−62 °C, CHCl₃, lock on C₆D₆): δ 3.5 (t, ¹J_{PH} = 358 Hz, PH₂), no signals with P–D coupling are observed); **MS**: m/z = 772.1 [Cp*TaCl₂(PH₂CH₂Fc)·3-NBA]⁺ (9.1 %), 655.0 [Cp*TaCl₃(PH₂CH₂Fc)]⁺ (62.3 %), 520.0 [TaCl₃(PH₂CH₂Fc)]⁺ (31.3 %), 423.0 [Cp*TaCl₂]⁺ (8.6 %), 289.1 [TaCl₃]⁺ (50.5 %), 232.0 [PH₂CH₂Fc]⁺ (17 %), 199.1 [CH₂Fc]⁺ (79 %); **IR** (cm^{−1}): 3079 w, 2994 w, 2964 w, 2909 m, 2371 w, 1644 m, 1491 m, 1455 m, 1437 m, 1411 m, 1374 s, 1261 m, 1149 w, 1104 s, 1070 m, 1044 m, 1025 m, 923 m, 867 s, 835 m, 813 m, 749 w, 703 w, 648 w, 599 w, 493 m, 422 w.

[Cp'TaCl₄(PH₂CH₂Fc)] (3b). PH₂CH₂Fc (0.14 g, 0.60 mmol) was added to a solution of [Cp'TaCl₄(THF)] (0.28 g, 0.59 mmol) in toluene (50 mL). After 12 h the solvent was evaporated in vacuum, and the brown residue washed with pentane (10 mL) and dried to give an orange powder. To obtain crystals, the latter was dissolved in CH₂Cl₂ (5 ml), and the solution filtered and cooled to −30 °C. After 1 d orange platelets had formed that rapidly decomposed to a grey powder in air by loss of solvent. Yield: 0.31 g (83 %); mp (orange powder): 166–167 °C (dec. >176 °C); Anal. calc. for C₁₇H₂₀Cl₄FePtA (633.93): C, 32.21; H, 3.18; Cl, 22.37. Found: C, 32.00; H, 2.27; Cl, 22.65 % [48].

¹H NMR (25 °C, C₆D₆): δ 2.40 (s, 3H, CH₃C₅H₄), 3.32 (m, 2H, PH₂CH₂), 3.74 and 3.83 (2 s, each 2H, PH₂CH₂C₅H₄), 3.86 (s, 5H, C₅H₅), 5.51 (d, ¹J_{PH} = 361 Hz, 2H, PH₂), 5.79 (m (pseudotriplets), ³J_{HHH}/⁴J_{HHH} = 5.2 Hz, 2H, CH₃C₅H₄), 6.33 (m (pseudotriplets), ³J_{HHH}/⁴J_{HHH} = 5.2 Hz, 2H, CH₃C₅H₄); **¹³C{¹H} NMR** (25 °C, C₆D₆): δ 16.2 (s, CH₃C₅H₄), 20.4 (d, ¹J_{PC} = 17.3 Hz, PH₂CH₂), 68.0 and 68.1 (2 s, C_A and C_B in PH₂CH₂C₅H₄), 69.9 (s, C₅H₅), 85.3 (d, ²J_{PC} = 11.1 Hz, C_C in PH₂CH₂C₅H₄), 125.2 and 126.2 (2 s, CH₃CCHCH and CH₃CCHCH in CH₃C₅H₄), 135.7 (s, CH₃CCHCH in CH₃C₅H₄); **³¹P{¹H} NMR** (25 °C, CDCl₃): δ 4.2 (br s, full width at half-maximum 0.3 ppm); **³¹P NMR** (25 °C, C₆D₆): δ 4.1 (br t, ¹J_{PH} = 366 Hz); **³¹P{¹H} NMR** (−63 °C, CDCl₃): δ 2.6 (s); **³¹P NMR** (−63 °C, CDCl₃): δ −2.7 (br t, ¹J_{PH} = 372 Hz); **MS**: m/z = 716.1 [Cp'TaCl₂(PH₂CH₂Fc)·3-NBA]⁺ (6.2 %), 599.1 [Cp'TaCl₃(PH₂CH₂Fc)]⁺ (6.6 %), 526.9 [Cp'TaCl(PH₂CH₂Fc)]⁺ (10.0 %), 295.0 [Cp'TaCl]⁺ (49 %), 232.1 [PH₂CH₂Fc]⁺ (100 %), 199.1 [CH₂Fc]⁺ (73 %), 154.1 [3-NBA]⁺ (96 %); **IR** (cm^{−1}): 3107 m, 3092 m, 2952 w, 2920 w, 2391 w, 1633 w, 1496 m, 1463 m, 1453 m, 1400 m, 1375 m, 1308 s, 1242 s, 1184 s, 1129 s, 1105 s, 1078 m, 1060 m, 1047 w, 1036 m, 1022 m, 1000 s, 984 s, 946 m, 925 m, 884 s, 862 m, 844 m, 825 m, 803 m, 759 w, 599 w, 496 m, 482 m, 429 w, 416 w.

[(Cp*TaCl₄)PH₂(η⁵-C₅H₄)₂Fe] (4a). A solution of (PH₂)₂fc (0.065 g, 0.26 mmol) in toluene (10 mL) was added to a solution of [Cp*TaCl₄] (0.24 g, 0.52 mmol) in toluene (15 mL). An orange precipitate formed slowly. After 24 h the solid was isolated by filtration, washed twice with *n*-pentane (2 x 10 mL) and dried for 3 h in vacuum. Yield: 0.24 g (79 %). The orange product is soluble in THF and slightly soluble in chlorinated organic solvents. Recrystallisation from CH₂Cl₂ gave red crystals of **4a**·2 CH₂Cl₂. Mp (powder): dec. >215 °C; Anal. calc. for C₃₀H₄₂Cl₈FeP₂Ta₂ (1165.98)·toluene: C, 35.32; H, 4.01; Cl, 22.54. Found: C, 35.80; H, 4.44, Cl, 21.89 %.

¹H NMR (25 °C, CDCl₃): δ 2.35 (s, 3H, CH₃ in toluene), 2.48 (s, 30H, C₅(CH₃)₅), 4.47 and 4.57 (2 s, each 4H, PH₂C₅H₄), ca. 6.0 (vbr d, full width at half-maximum 0.1 ppm, ¹J_{PH} ≈ 340 Hz, PH₂), 7.18 (m, 5H, C₆H₅ in toluene); **¹H NMR** (−60 °C, CDCl₃): signal at δ 6.33 (d, ¹J_{PH} = 367 Hz, 4H, PH₂); **¹³C{¹H} NMR** (25 °C, CDCl₃): δ 13.4 (s, C₅(CH₃)₅), 22.2 (s, CH₃ in toluene), 73.8 (d, ³J_{PC} = 6.2 Hz, C_A in PH₂C₅H₄), 76.0 (d, ²J_{PC} = 7.8 Hz, C_B in PH₂C₅H₄), 133.4 (s, C₅(CH₃)₅), 126.0, 128.9, 129.7 and 138.6 (4 s, CH in toluene), C_C in PH₂C₅H₄ not observed; **³¹P{¹H} NMR** (25 °C, CDCl₃): no signal; **³¹P NMR** (−60 °C, CDCl₃): δ −7.6 (t, ¹J_{PH} = 367 Hz). **MS** (FAB, 700 < m/z < 1300): m/z = 1057.6 [M−3Cl]⁺ (4 %), 923.7 [M−Cp*−3Cl]⁺ (14 %), 823.6 [M−2Cp*−2Cl]⁺ (19 %), 757.8 [M−2Cp*−4Cl]⁺ (13 %); **IR** (cm^{−1}): 3090 w, 2994 w, 2962 w, 2911 m, 2365 w, 1602 w, 1492 m, 1454 w, 1436 m, 1418 w, 1375 m, 1261 w, 1181 m, 1171 w, 1073 w, 1053 m, 1028 m,

889 m, 865 s, 830 m, 809 w, 740 m, 697 m, 598 w, 487 m, 468 w, 451 w, 427 m.

[(Cp*TaCl₄)PH₂(η⁵-C₅H₄)₂Fe] (4b). A solution of (PH₂)₂fc (0.065 g, 0.26 mmol) in toluene (10 mL) was added to a solution of [Cp*TaCl₄(THF)] (0.25 g, 0.52 mmol) in toluene (40 mL). A colour change from orange to brown occurred and a dark brown precipitate formed. After 24 h the solid was isolated by filtration, washed with toluene (2 × 10 mL) and *n*-pentane (2 × 10 mL). The solid was dried for 3 h in vacuum. The product is slightly soluble in THF and Et₂O, but insoluble in most other organic solvents. The solid was extracted with hot Et₂O to yield the product as a yellow powder. Yield: 0.26 g (95 %); mp: ca. 270 °C (dec. >177 °C); Anal. calc. for C₂₂H₂₆Cl₈FeP₂Ta₂ (1053.77) · 0.85 toluene: C, 29.65; H, 2.92; Cl, 25.05. Found: C, 29.70; H, 2.65; Cl, 24.75 %.

¹H NMR (25 °C, CDCl₃): δ 2.30 (s, CH₃ in toluene), 2.83 (s, 6H, CH₃C₅H₄), 4.38 (s, 8H, Fe(C₅H₄)₂), 6.43 and 6.86 (2 s, each 4H, CH₃C₅H₄), 7.20–7.07 (2 m, C₆H₅ in toluene), PH₂ not observed. ¹H NMR (–50 °C, CDCl₃): δ 2.30 (s, CH₃ in toluene), 2.72 (s, 6H, CH₃C₅H₄), 4.65–4.14 (m, 8H, PH₂C₅H₄), 6.54 (d, ¹J_{PH} = 375 Hz) and 6.57 (d, ¹J_{PH} = 376 Hz) (PH₂, total 4H, ratio 1:2, different rotamers), 6.50 and 6.93 (2 s, each 4H, CH₃C₅H₄), 7.21–7.11 (2 m, C₆H₅ in toluene); ¹³C{¹H} NMR (25 °C, THF-d₈): δ 21.4 (s, CH₃C₅H₄), 73.2 (PH₂C₅H₄), 125.9, 128.8, 125.9, 125.1 (4 s, CH₃CCHCH and CH₃CCHCH in CH₃C₅H₄), 138.3 (s, CH₃CCHCH in CH₃C₅H₄), the intensity of the signals is rather low due to the low solubility, and some signals of **4b** (fc group) are obscured by the solvent (ca. 67 ppm); ³¹P{¹H} NMR (25 °C, THF/CDCl₃): δ no signal; ³¹P{¹H} NMR (–62 °C, THF/CDCl₃): δ –3.3 (s, 100 %), rotamers at –1.9 (s, 93 %), –1.0 (s, 23 %) and –0.3 (s, 9 %); ³¹P{¹H} NMR (–60.5 °C, THF-d₈): δ –8.4 (s, 100 %), rotamers at –7.0 (s, 50 %), and –5.4 (s, 8 %); ³¹P NMR (–60.5 °C, THF/CDCl₃): δ –3.3 (t, ¹J_{PH} = 375 Hz), rotamer at –1.9 (t, ¹J_{PH} = 373 Hz); ³¹P{¹H} NMR (–60.5 °C, THF-d₈): δ –8.4 (t, ¹J_{PH} = 376 Hz), rotamer at –7.0 (t, ¹J_{PH} = 374 Hz); the ³¹P NMR spectra show the signals of (PH₂)₂fc as impurity. MS (FAB, 500 < m/z < 1500): m/z = 946.5 [M–3Cl]⁺ (12.8 %), 867.8 [M–Cp*–3Cl]⁺ (5.4 %), 787.8 [M–2Cp*–3Cl]⁺ (9.3 %), 752.6 [M–2Cp*–4Cl]⁺ (3.0 %), 714.9 [M–2Cp*–5Cl]⁺ (49.4 %); IR (cm^{–1}): 3117 m, 3090 m, 3019 w, 2959 w, 2914 w, 2387 w, 2364 w, 1602 w, 1495 m, 1450 m, 1419 w, 1401 w, 1386 m, 1375 m, 1248 w, 1183 m, 1174 m, 1078 m, 1048 m, 1030 m, 936 w, 891 m, 864 s, 836 m, 737 m, 697 m, 636 w, 610 w, 594 w, 490 m, 459 m, 424 m.

[Cp*TaCl₄{PH(CH₂Fc)₂}] (5a). PH(CH₂Fc)₂ (0.15 g, 0.35 mmol) was added to a solution of [Cp*TaCl₄] (0.16 g, 0.35 mmol) in toluene (20 mL). After 24 h the solution was filtered through Celite, and the solvent was evaporated in vacuum. A brown oily residue was obtained, which was stirred in *n*-pentane until it solidified. The ochre powder was washed with *n*-pentane (10 mL) and dried. Yield: 0.28 g (90 %). Recrystallisation from toluene gave dark red crystals of **5a** · toluene. Mp (crystals): dec. 117–119 °C; Anal. calc. for C₃₂H₃₈Cl₄Fe₂P₂Ta [888.09] · toluene: C, 47.79; H, 4.73; Cl, 14.47. Found: C, 46.90; H, 3.09, Cl, 13.93 % [48].

¹H NMR (25 °C, CDCl₃): δ 2.50 (s, 15H, C₅(CH₃)₅), 3.05 and 3.56 (2 br m, each 2H, PCH₂Fc), 4.07 (s, 10H, C₅H₅), 3.88 (s, 2H, C₅H₄), 4.14 (s, 2H, C₅H₄), 4.03 (s, 4H, C₅H₄), 4.86 (br d, ¹J_{PH} = 373 Hz, 1H, PH); ¹³C{¹H} NMR (25 °C, CDCl₃): δ 13.4 (s, C₅(CH₃)₅), 23.7 (d, ¹J_{PC} = 15.0 Hz, PH₂CH₂), 68.2 and 68.5 (2 s, C_A and C_B in PH₂CH₂C₅H₄), 69.5 (s, C₅H₅), 70.2 (2 s, Δδ = 0.058, C_A and C_B in PH₂CH₂C₅H₄), 85.6 (d, ²J_{PC} = 8 Hz, C_C in PH₂CH₂C₅H₄), 133.1 (s, C₅(CH₃)₅); ¹³C{³¹P, ¹H} NMR (25 °C, CDCl₃): δ 13.4 (s, C₅(CH₃)₅), 23.7 (s, PH₂CH₂), 68.2 and 68.5 (2 s, C_A and C_B in PH₂CH₂C₅H₄), 69.5 (s, C₅H₅), 70.2 (2 s, Δδ = 0.058, PCCC₄ in PH₂CH₂C₅H₄), 85.6 (s, C_C in PH₂CH₂C₅H₄), 133.1 (s, C₅(CH₃)₅); ³¹P{¹H} NMR: see Table 3; MS (FAB, 200 < m/z < 1000): m/z = 642.6 [TaCl₄{PH(CH₂Fc)₂}]⁺ (2.8 %), 611.1 [Cp*TaCl₄·3-NBA]⁺ or [Ta{PH(CH₂Fc)₂}]⁺ (1.8 %), 430.0 [PH(FeCH₂)₂]⁺ (30 %), 231.1 [PHCH₂Fc]⁺ (23 %); IR (cm^{–1}): 3921 w, 3427 m, 3088 m, 2993 w, 2963 m, 2913 w, 2386 w, 1633 br w, 1494 m, 1460 m, 1437 m, 1403 m, 1372 s, 1261 m, 1235 m, 1201 w, 1178 w, 1104 s, 1040 m, 1023 m, 1000 m, 922 m, 872 m, 860 w, 822 s, 739 m, 697 m, 597 w, 502 s, 484 m, 467 w, 425 m.

[Cp*TaCl₄{PH(CH₂Fc)₂}] (5b). PH(CH₂Fc)₂ (0.15 g, 0.35 mmol) was added to a solution of [Cp*TaCl₄(THF)] (0.16 g, 0.34 mmol)

in toluene (20 mL). After 24 h the solution was filtered through Celite, and the solvent was evaporated in vacuum. The remaining ochre powder was washed with pentane (10 mL) and dried. The residue was dissolved in CH₂Cl₂ (5 mL), and the solution filtered and kept at r.t. After 1 month intergrown needles had formed. Yield: 0.24 g (85 %); mp: dec. >174 °C; Anal. calc. for C₂₈H₃₀Cl₄Fe₂P₂Ta [831.94]: C, 40.42; H, 3.64; Cl, 17.05. Found: C, 41.20; H, 2.33, Cl, 16.06 % [48].

¹H NMR (25 °C, CDCl₃): δ 2.85 (s, 3H, C₅H₄CH₃), 3.11 and 3.58 (2 m, each 2H, PCH₂Fc), 4.07 (s, 10H, C₅H₅), 4.05 and 4.14 (2 s, each 4H, C₅H₄), 4.99 (d of quint, 1H, ¹J_{PH} = 378 Hz, ³J_{HH} = 3.5 Hz, PH), 6.35 (m (pseudotriplets), ³J_{HH}/⁴J_{HH} = 5.2 Hz, 2H) and 6.83 (m (pseudotriplets), ³J_{HH}/⁴J_{HH} = 5.2 Hz, 2H) (both CH₃C₅H₄); ¹³C{¹H} NMR (25 °C, CDCl₃): δ 16.5 (s, CH₃C₅H₄), 23.7 (br s, PH₂CH₂), 68.4 and 68.7 (2 s, C_A and C_B in PH₂CH₂C₅H₄), 69.6 (s, C₅H₅), 70.1 (s, C_C in PH₂CH₂C₅H₄), 125.1 and 125.8 (2 s, CH₃CCHCH and CH₃CCHCH in CH₃C₅H₄), 128.9 (s, CH₃CCHCH in CH₃C₅H₄); ³¹P{¹H} NMR: see Table 2; MS (FAB, 400 < m/z < 1000): m/z = 946.7 [Cp*TaCl₄{P(CH₂Fc)₂}·3-NBA]⁺ (6.7 %), 832.8 [Cp*TaCl₄{PH(CH₂Fc)₂}]⁺ or [TaCl₄{P(CH₂Fc)₂}·3-NBA]⁺ (1.2 %), 796.8 [Cp*TaCl₄{PH(CH₂Fc)₂}]⁺ (8.6 %), 752.7 [TaCl₄{PH(CH₂Fc)₂}]⁺ (2.1 %), 716.0 [TaCl₄{PH(CH₂Fc)₂}]⁺ (2.6 %); IR (cm^{–1}): 3107 m, 3092 m, 2961 w, 2920 m, 2910 m, 2391 w, 1634 br w, 1496 m, 1463 m, 1453 m, 1400 m, 1375 m, 1261 m, 1247 m, 1234 m, 1213 w, 1105 s, 1078 m, 1047 m, 1038 m, 1023 s, 1002 m, 939 m, 925 m, 854 s, 862 m, 845 m, 825 s, 803 s, 760 w, 730 w, 694 w, 598 w, 497 s, 482 s, 428 w, 417 w, 404 w.

Acknowledgment. We gratefully acknowledge financial support by the Deutsche Forschungsgemeinschaft and a generous supply of tetrakis(hydroxymethyl)phosphonium chloride by Cytec. P.Z. acknowledges the financial support of the University of Siena (PAR progetti, 2005).

References

- [1] Eds. E. W. Abel, F. G. A. Stone, G. Wilkinson, *Comprehensive Organometallic Chemistry II 1995*, Volumes 4 and 5, Pergamon Press.
- [2] W. Henderson, S. R. Alley, *J. Organomet. Chem.* **2002**, *656*, 120.
- [3] N. J. Goodwin, W. Henderson, B. K. Nicholson, J. Fawcett, D. R. Russell, *J. Chem. Soc., Dalton Trans.* **1999**, 1785.
- [4] N. J. Goodwin, W. Henderson, B. K. Nicholson, *Chem. Commun.* **1997**, 31.
- [5] P. P. Power, R. A. Bartlett, M. M. Olmstead, G. A. Sigel, *Inorg. Chem.* **1987**, *26*, 1941.
- [6] P. P. Power, B. Twamley, C. Hwang, N. J. Hardman, *J. Organomet. Chem.* **2000**, *609*, 152.
- [7] K. V. Katti, K. R. Prabhu, N. Pillarsetty, H. Gali, *J. Am. Chem. Soc.* **2000**, *122*, 1554.
- [8] R. M. Hiney, L. J. Higham, H. Müller-Bunz, D. G. Gilheany, *Angew. Chem.* **2006**, *118*, 7406; *Angew. Chem. Int. Ed.* **2006**, *45*, 7248.
- [9] M. M. Dell'Anna, U. Englert, M. Latronica, P. L. Luis, P. Mastroianni, D. G. Papa, C. F. Nobile, M. Peruzzini, *Inorg. Chem.* **2006**, *45*, 6892.
- [10] R. Kalio, P. Lönnecke, E. Hey-Hawkins, *J. Organomet. Chem.* (submitted).
- [11] T. Höcher, S. Blaurock, E. Hey-Hawkins, *Eur. J. Inorg. Chem.* **2002**, 1174; T. Höcher, S. Blaurock, E. Hey-Hawkins, *Phosphorus, Sulfur* **2002**, *177*, 2169.
- [12] A. Togni, T. Hayashi, *Ferrocenes. Homogeneous Catalysis, Organic Synthesis Materials Science*, VCH Weinheim, **1995**.
- [13] (a) J. C. Leblanc, C. Moïse, *J. Organomet. Chem.* **1989**, *364*, C3; (b) R. T. Baker, J. C. Calabrese, R. L. Harlow, I. D. Williams, *Organometallics* **1993**, *12*, 830; (c) G. I. Nikonov, L. G.

- Kuzmina, P. Mountford, D. A. Lemenovskii, *Organometallics* **1995**, *14*, 3588; (d) G. Bonnet, O. Lavastre, J. C. Leblanc, C. Moïse, *New J. Chem.* **1988**, *12*, 551; (e) C. Poulard, G. Boni, P. Richard, C. Moïse, *J. Chem. Soc. Dalton Trans.* **1999**, 2725; (f) O. Lavastre, G. Bonnet, G. Boni, M. M. Kubicki, C. Moïse, *J. Organomet. Chem.* **1997**, *547*, 141; (g) P. Sauvageot, O. Blacque, M. M. Kubicki, S. Juge, C. Moïse, *Organometallics* **1996**, *15*, 2399; (h) S. Challet, O. Lavastre, C. Moïse, J.-C. Leblanc, B. Nuber, *New J. Chem.* **1994**, *18*, 1155; (i) P. Oudet, M. M. Kubicki, C. Moïse, *Acta Crystallogr.* **1995**, *C51*, 811.
- [14] (a) G. A. A. Hadi, K. Fromm, S. Blaurock, S. Jelonek, E. Hey-Hawkins, *Polyhedron* **1997**, *16*, 721; (b) U. Segerer, R. Felsberg, S. Blaurock, G. A. Hadi, E. Hey-Hawkins, *Phosphorus, Sulfur* **1999**, *477*, 144.
- [15] (a) G. I. Nikonov, Y. K. Grishin, D. A. Lemenovskii, N. B. Kazennova, L. G. Kuzmina, J. A. K. Howard, *J. Organomet. Chem.* **1997**, *547*, 183; (b) G. I. Nikonov, D. A. Lemenovskii, K. Y., Dorogov, A. V. Churakov, *Polyhedron* **1999**, *18*, 1159.
- [16] P. J. Domaille, B. M. Foxmann, T. J. McNeese, S. S. Wreford, *J. Am. Chem. Soc.* **1980**, *102*, 4114.
- [17] J. B. Bonanno, P. T. Wolczanski, E. B. Lobkovsky, *J. Am. Chem. Soc.* **1994**, *116*, 11159.
- [18] N. Etkin, M. T. Benson, S. Courtenay, M. J. McGlinchey, A. D. Bain, D. W. Stephan, *Organometallics* **1997**, *16*, 3504.
- [19] C. C. Cummins, R. R. Schrock, W. M. Davis, *Angew. Chem.* **1993**, *105*, 758.
- [20] J. A. Labinger, in *Comprehensive Organometallic Chemistry* (Edited by Wilkinson, G.) **1982**, Pergamon Press, Oxford, Vol. 3, Chapter 25, p. 705 ff.
- [21] N. N. Greenwood, A. Earnshaw, *Die Chemie der Elemente*, **1988**, VCH Verlagsgesellschaft, Weinheim.
- [22] (a) E. Hey-Hawkins, *Chem. Rev.* **1994**, *94*, 1661; (b) D. W. Stephan, *Angew. Chem.* **2000**, *112*, 322 (and references therein).
- [23] (a) E. Hey-Hawkins, K. Fromm, *Polyhedron* **1995**, *14*, 2825; (b) R. Felsberg, S. Blaurock, S. Jelonek, T. Gelbrich, R. Kirmse, A. Voigt, E. Hey-Hawkins, *Chem. Ber./Recueil* **1997**, *130*, 807.
- [24] (a) M. J. Bunker, A. de Cian, M. L. H. Green, *J. Chem. Soc. Chem. Commun.* **1977**, 59; (b) M. J. Bunker, A. de Cian, M. L. H. Green, J. J. E. Moreau, N. Siganporia, *J. Chem. Soc., Dalton Trans.* **1980**, 2155; (c) W. A. Herrmann, W. Kalcher, H. Biersack, I. Bernal, M. Creswick, *Chem. Ber.* **1981**, *114*, 3558; (d) R. J. Burt, G. Leigh, D. L. Hughes, *J. Chem. Soc. Dalton Trans.* **1981**, 793; (e) A. Nakamura, T. Okamoto, H. Yasuda, *Organomet. Synth.* **1988**, *4*, 20 (and references therein).
- [25] R. J. Burt, G. J. Leigh, *J. Organomet. Chem.* **1978**, *148*, C19.
- [26] M. I. Alcalde, J. de la Mata, M. Gomez, P. Royo, F. Sanchez, *J. Organomet. Chem.* **1995**, *492*, 151.
- [27] J. C. Fettingner, D. W. Keogh, R. Poli, *Inorg. Chem.* **1995**, *34*, 2343.
- [28] S. Blaurock, E. Hey-Hawkins, *Z. Anorg. Allg. Chem.* **2002**, *628*, 2515.
- [29] C. Spang, F. T. Edelmann, M. Noltemeyer, H. W. Roesky, *Chem. Ber.* **1989**, *122*, 1247.
- [30] S. I. M. Paris, F. R. Lemke, R. Sommer, P. Lönnecke, E. Hey-Hawkins, *J. Organomet. Chem.* **2005**, *690*, 1807.
- [31] S. I. M. Paris, J. L. Petersen, E. Hey-Hawkins, M. P. Jensen, *Inorg. Chem.* **2006**, *45*, 5561.
- [32] R. Sommer, *Dissertation*, Univ. Leipzig, Leipzig, Germany, **2002**.
- [33] E. Hey-Hawkins, P. K. Baker, R. Sommer, P. Lönnecke, *Inorg. Chem. Comm.* **2002**, *5*, 115.
- [34] R. Sommer, P. Lönnecke, J. Reinhold, P. K. Baker, E. Hey-Hawkins, *Organometallics* **2005**, *24*, 5256.
- [35] R. Kalio, P. Lönnecke, J. Reinhold, E. Hey-Hawkins, *Organometallics* **2007**, *26*, 3884.
- [36] A. J. Downard, N. J. Goodwin, W. J. Henderson, *J. Organomet. Chem.* **2003**, *676*, 62.
- [37] a) I. R. Butler, U. Griesbach, P. Zanello, M. Fontani, D. Hibbs, M. B. Hursthouse, K. L. M. Abdul Malik, *J. Organomet. Chem.* **1998**, *565*, 243 (and references therein); b) F. Barrière, R. U. Kirss, W. E. Geiger, *Organometallics* **2005**, *24*, 48.
- [38] G. Ferguson, C. Glidewell, G. Opromolla, C. M. Zakaria, P. Zanello, *J. Organomet. Chem.* **1996**, *506*, 129.
- [39] E. A. Quadrelli, H.-B. Kraatz, R. Poli, *Inorg. Chem.* **1996**, *35*, 5154 (and references therein).
- [40] P. Zanello, *Inorganic Electrochemistry. Theory, Practice and Application*, RSC, United Kingdom, **2003**.
- [41] a) M. Ferrali, S. Bambagioni, A. Ceccanti, D. Donati, G. Giorgi, M. Fontani, F. Laschi, P. Zanello, M. Casolaro, A. Pietrangelo, *J. Med. Chem.* **2002**, *45*, 5776; (b) P. Mura, M. Camalli, L. Messori, F. Piccioli, P. Zanello, M. Corsini, *Inorg. Chem.* **2004**, *43*, 3863; (c) M. Ravera, S. Baracco, C. Cassino, P. Zanello, D. Osella, *Dalton Trans.* **2004**, 2347.
- [42] H. Günther, *NMR-Spektroskopie: eine Einführung in die Protonenresonanz-Spektroskopie und ihre Anwendung in der Chemie*, Thieme Stuttgart, New York, 2. Aufl. **1983**, 198.
- [43] M. J. Burk, M. Gross, *Tetr. Lett.* **1994**, *35*, 9363.
- [44] R. D. Sanner, S. D. Carter, W. J. Bruton Jr., *J. Organomet. Chem.* **1982**, *240*, 157.
- [45] F. Fabrizi de Biani, M. Corsini, P. Zanello, H. Yao, M. E. Bluhm, R. N. Grimes, *J. Am. Chem. Soc.* **2004**, *126*, 11360.
- [46] SADABS: G. M. Sheldrick, *SADABS, Program for Scaling and Correction of Area-detector Data*, Göttingen, **1997**.
- [47] SHELX97: G. M. Sheldrick, *SHELXS97 and SHELXL97 – Programs for Crystal Structure Analysis*. University of Göttingen, **1998**.
- [48] Elemental analysis repeatedly gave lower H values than calculated even for different samples.